Catalysis Today 151 (2010) 257–265

Contents lists available at ScienceDirect

Catalysis Today

journal homepage: www.elsevier.com/locate/cattod

Deactivation of accelerated engine-aged and field-aged Fe–zeolite SCR catalysts

Todd J. Toops [a,*], Ke Nguyen [b], Adam L. Foster [b], Bruce G. Bunting [a], Nathan A. Ottinger [a], Josh A. Pihl [a], Edward W. Hagaman [a], Jian Jiao [a]

[a] Oak Ridge National Laboratory, P.O. Box 2008, Oak Ridge, TN 37831, USA
[b] Mechanical, Aerospace, and Biomedical Engineering Dept., University of Tennessee, Knoxville, TN 37996, USA

ARTICLE INFO

Article history:
Available online 23 February 2010

Keywords:
Fe–zeolite SCR catalyst
Accelerated aging protocols
Field-aged catalysts
XRD
BET
NMR

ABSTRACT

A single-cylinder diesel engine with an emissions control system – diesel oxidation catalyst (DOC), Fe–zeolite selective catalytic reduction (SCR) catalyst, and diesel particulate filter (DPF) – was used to perform accelerated thermal aging of the SCR catalyst. Cyclic aging is performed at SCR inlet temperatures of 650, 750 and 850 °C for up to 50 aging cycles. To assess the validity of the implemented accelerated thermal aging protocol, a field-aged SCR catalyst of similar formulation was also evaluated. The monoliths were cut into sections and evaluated for NO_x performance in a bench-flow reactor. While the rear section of both the field-aged and the accelerated engine-aged SCR catalysts maintained high NO_x conversion, 75–80% at 400 °C, the front section exhibited a drastic decrease to only 20–35% at 400 °C. This two-tiered deactivation was also observed for field-aged samples that were analyzed in this study. To understand the observed performance changes, thorough materials characterization was performed which revealed two primary degradation mechanisms. The first mechanism is a general Fe–zeolite deterioration which led to surface area losses, dealumination of the zeolite, and Fe_2O_3 crystal growth. This degradation accelerated above 750 °C, and the effects were generally more severe in the front of the catalyst. The second deactivation mechanism is linked to trace levels of Pt that are suspected to be volatizing from the DOC and depositing on the front section of the SCR catalyst. Chemical evidence of this can be seen in the high levels of NH_3 oxidation (80% conversion at 400 °C), which coincides with the decrease in performance.

1. Introduction

Of the most common technologies for reducing NO_x from lean burn engines – lean NO_x traps (LNT), hydrocarbon-based lean NO_x catalysis (LNC) and urea-based selective catalytic reduction (SCR) – SCR has been identified as one of the most promising candidates for NO_x abatement for meeting stringent diesel emissions regulations [1–13]. These zeolite-based systems are particularly attractive because they do not rely on precious metals, have high tolerance to sulfur, and have good activity over a wide temperature range. A current concern of these catalysts is their high temperature durability in the presence of steam. These conditions are encountered when the diesel particulate filter (DPF) is regenerated and the trapped soot is oxidized at 600–700 °C. If uncontrolled, these thermal excursions, which are initiated over an upstream diesel oxidation catalyst (DOC), can lead to the degradation and loss of performance of the SCR catalysts.

The majority of research on the durability of zeolite-based SCR catalysts utilized furnace-based hydrothermal aging up to 700 °C [5,14,15]. Generally, modern metal-exchanged zeolites have shown durability under these controlled conditions with less than 10% decrease in NO_x reduction activity. Even under conditions where activity is maintained, there is evidence of a decrease in surface area and dealumination, which occurs when the Al^{3+} ion in the SiO_2–Al_2O_3 tetrahedral framework migrates out of the structure. This typically manifests itself as a decrease in NH_3 adsorption capacity and the loss of surface acidity [16]. Aging beyond these typical DPF regeneration temperatures, circa 600–700 °C, the zeolites begin to dramatically breakdown structurally [16]. Therefore, thermal stability of the zeolite at temperatures experienced during normal engine operation and active regeneration of the diesel particulate filter is one of the vital factors for SCR catalyst selection and application.

While considerable efforts have been carried out to elucidate the deactivation mechanisms of SCR catalysts as a result of furnace-based hydrothermal aging, it is unclear if this procedure effectively replicates typical "on-road" aging conditions. The purpose of the present study is to gain a better understanding of the thermal durability and deactivation mechanisms of zeolite-based SCR catalyst systems by performing accelerated thermal aging on a

* Corresponding author at: Oak Ridge National Laboratory, P.O. Box 2008, Oak Ridge, Tennessee 37831, USA. Tel.: +1 865 946 1207; fax: +1 865 946 1354.
E-mail address: toopstj@ornl.gov (T.J. Toops).

0920-5861/$ – see front matter © 2010 Elsevier B.V. All rights reserved.
doi:10.1016/j.cattod.2010.01.019

commercial Fe–zeolite catalyst using an engine-based emissions control system approach. In the implemented accelerated thermal aging protocol, the aging of the SCR catalyst is achieved by increasing the exhaust temperature to replicate periodic DPF regeneration. The NO_x performance of the engine-aged catalysts is then evaluated on a bench reactor to determine the extent of catalyst degradation, and material characterization is performed to ascertain the deactivation mechanisms associated with engine-aging. Finally, the results obtained with the accelerated engine-aged catalysts are compared to those of the field-aged catalysts of a similar formulation, to ensure that the accelerated protocol replicates field results. Thus, the objectives of the proposed investigation are twofold: (i) to ascertain the deactivation mechanisms that led to the degradation in NO_x performance of the aged catalysts, and (ii) to assess the validity of the implemented accelerated engine-aging protocol in replicating the aging conditions observed in the field-aged Fe–zeolite SCR catalysts.

2. Experimental

2.1. Engine bench

Accelerated thermal aging is carried out on a bench-mounted naturally aspirated, direct injection 517 cm^3 single-cylinder Hatz diesel engine. An electric induction motor and drive are used to control engine speed and load, producing consistent and repeatable exhaust temperatures during the periodic DPF regeneration. The emissions control system, consisting of an upstream DOC, a SCR catalyst and a downstream DPF, is fitted to the exhaust manifold of the bench-mounted diesel engine as shown in Fig. 1. The ammonia/exhaust mixer aids the distribution of the injected NH_3 with the incoming engine exhaust prior to entering the SCR catalyst.

A fuel injection system installed approximately 0.3 m downstream of the exhaust manifold is used to inject fuel into the engine exhaust to initiate the exotherm for DPF regeneration. The fuel is pumped through a 1.6 mm stainless steel tube into a vaporizer using a FMI (Fluid Metering, Inc.) laboratory pump. The fuel is vaporized by a cartridge heater maintained at 375 °C. The evaporated fuel is then injected into the exhaust gas through a nozzle using compressed air at a flow rate of 1000 sccm/min as a sweeper gas.

Each catalyst is mounted in a 7.6 cm diameter steel can. Before being placed in the cans, the catalysts are wrapped in a vermiculite-coated fiber mat which provides insulation and prevents gas slippage around the catalyst. The exhaust pipe is also wrapped in insulation to minimize heat losses from the emissions control system.

Engine speed is maintained at 1500 RPM, corresponding to a gas hourly space velocity (GHSV) of 30,000 h^{-1} in the SCR catalyst. To minimize the effect of fuel-borne sulfur on the emissions control system, the fuel used is BP-15, a #2 ultra low sulfur diesel fuel produced by British Petroleum, containing less than 15 ppm sulfur.

2.2. Accelerated thermal aging protocol

Accelerated aging of Fe–zeolite SCR catalysts is carried out during periodic active regeneration of the DPF at target exhaust gas temperatures of 650, 750 and 850 °C at the SCR inlet. Since engine-out exhaust temperature averages 350 °C, the desired aging temperatures are achieved by injecting vaporized fuel into the engine exhaust immediately downstream of the exhaust manifold. Fuel is injected for 25 min per cycle and continued for up to 50 cycles. The fuel flow rates are calibrated and adjusted to provide specific SCR catalyst temperatures for the specific time. The fuel flow rate is increased stepwise in 5-min increments until the targeted aging temperature at the SCR inlet is reached. In such a manner uncontrolled DPF regenerations can be avoided, which could possibly lead to excessively high temperatures and subsequent catastrophic failure of the DPF.

2.3. Catalysts

Fresh Fe–zeolite SCR catalysts and a field-aged catalyst of similar formulation operated for 2 years on a diesel transit bus were obtained from the manufacturer, Catalytic Solutions. The fresh SCR catalysts primarily consist of Fe–zeolite, but also contain an oxygen storage component: 2–3 wt% ceria–zirconia. These active materials were loaded on a 400 cells per square inch (cpsi) cordierite substrate of 7.6 cm in diameter and 15.2 cm in length. The upstream DOC is used to generate exotherms from which the thermal aging of the SCR and the regeneration of the DPF are implemented. The DOC is 7.6 cm in diameter and 7.6 cm long with a cell density of 400 cpsi and is composed of Pt/Al_2O_3 in the washcoat; whereas the downstream

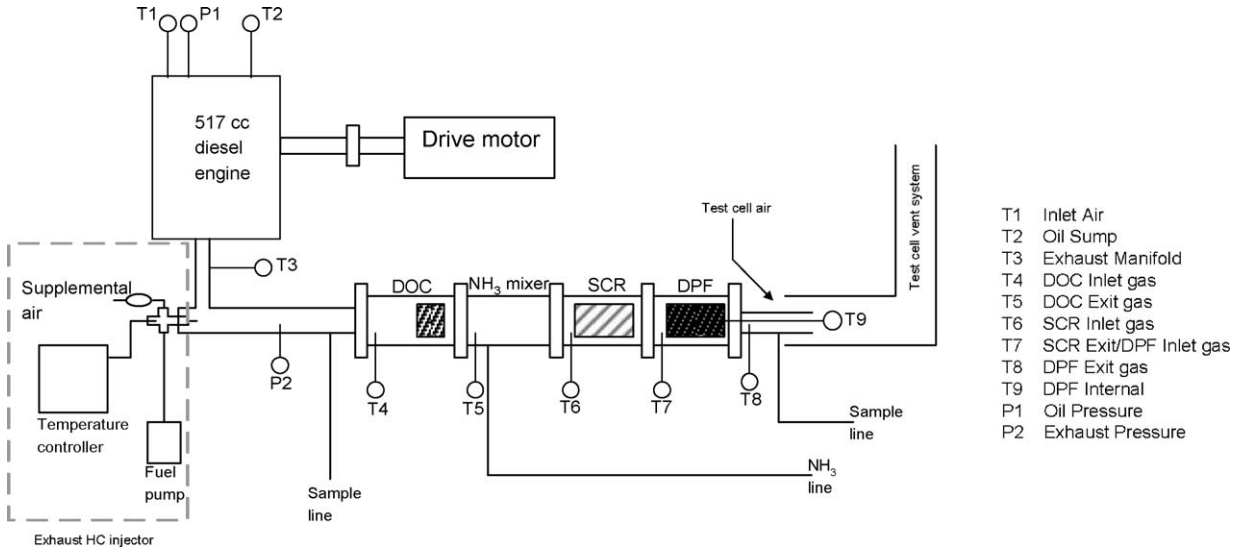

Fig. 1. Schematic of engine bench and emissions control system.

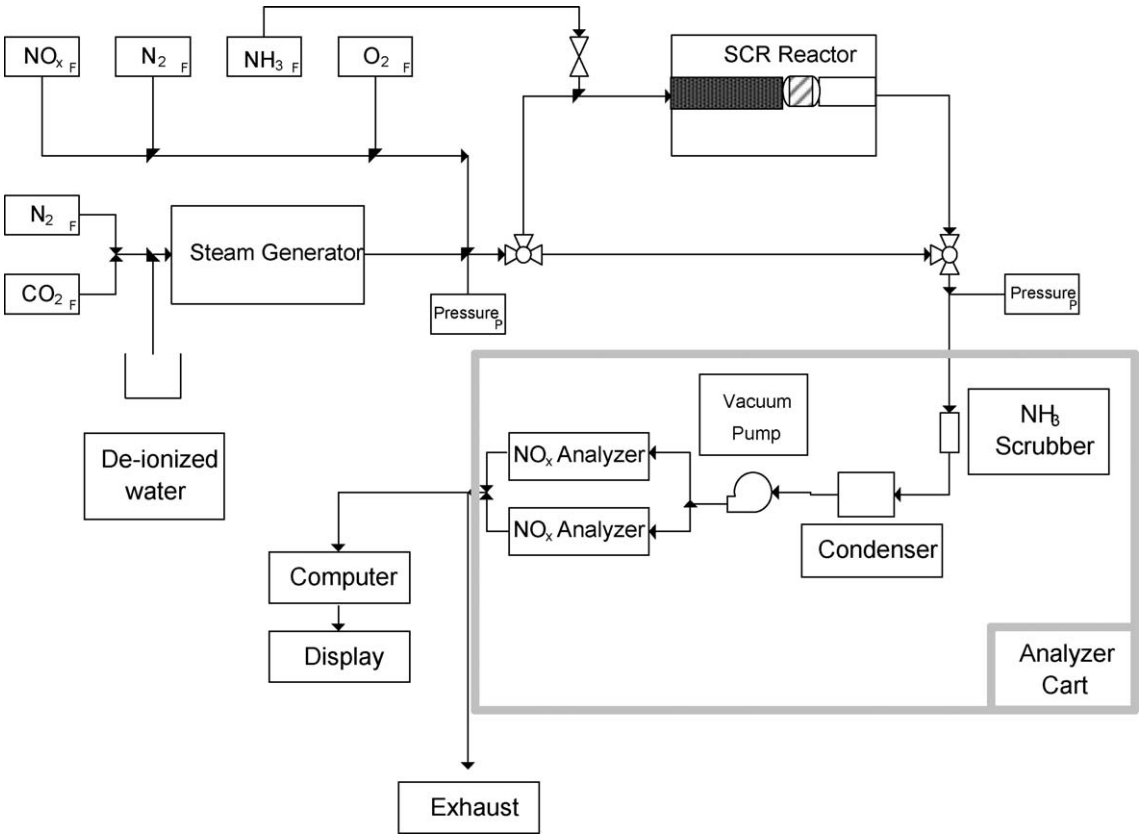

Fig. 2. Schematic of bench-flow reactor system.

catalyzed DPF is 7.6 cm diameter and 15.2 cm long and has a cell density of 200 cpsi.

2.4. Bench-flow reactor for NO_x performance evaluation

The NO_x performance of fresh, engine-aged and field-aged SCR catalysts is measured in a bench-flow reactor, shown schematically in Fig. 2. The bench-flow reactor has been described in detail elsewhere [17,18], therefore, only a brief description is given here. The SCR reactor is a 43 cm long quartz tube with a 2.5 cm outside diameter placed inside a Lindberg Mini-mite furnace. The upstream section of the quartz tube is filled with quartz beads of 5 mm in diameter to ensure good mixing and uniform heating of the incoming gas. A 400 cpsi, cored sample of 2.2 cm diameter and 7.6 cm length wrapped in FiberFlax fiber strands to prevent gas bypass is positioned in the downstream section of the quartz tube. Cored samples taken from fresh, front, and rear sections of engine-aged and field-aged SCR catalysts are evaluated using simulated diesel exhaust gases comprising 5% CO_2, 5% H_2O, 14% O_2, 350 ppm NO, 350 ppm NH_3 and N_2 balance at a GHSV of 30,000 h^{-1} over a temperature range of 200–600 °C. NH_3 is introduced upstream of the SCR reactor through a separate heated line; once mixed with the other gases the lines are maintained at 200 °C to prevent the formation of ammonium nitrates. The inlet and exit concentrations of NO and total NO_x are independently measured with two chemiluminescent NO_x analyzers. Upstream of the NO_x analyzers, an ammonia scrubber (Perma Pure, LLC) is installed to prevent NH_3 from interfering with NO_x measurements.

Hydrothermal aging of SCR catalysts is also carried out in the bench-flow reactor at a GHSV of 30,000 h^{-1}. The composition of the simulated exhaust gases used during hydrothermal aging is similar to that used during NO_x performance evaluation but there is no NO_x or NH_3 and 28 ppm SO_2 is included in the feed.

2.5. Materials characterization

A number of analytical characterization techniques were used in this study to identify physical and chemical changes to the Fe–zeolite SCR catalysts as the result of aging. They include powder X-ray diffraction (XRD), scanning electron microscopy (SEM), BET surface area measurements, and solid state nuclear magnetic resonance (NMR) spectroscopy. Together these techniques provide bulk, surface, elemental, and chemical characterization of the catalysts. This information will facilitate the comparison of engine-aged and field-aged SCR catalysts to validate the accelerated thermal aging protocol and identification of aging mechanisms.

In powder XRD, the zeolite washcoat is scraped from the substrate and ground into a fine powder. The material is placed on a zero background carbon plate of approximately 3.8 cm in diameter. Scans are taken using a Philips wide angle XRD with a CuKα radiation source over a 2θ angle of 5–75 in a scan mode of 0.02° in 2 s.

Surface topography is obtained for each SCR catalyst using a Leo 1525 field emission SEM outfitted with a Link Oxford EDS detector. SCR catalyst samples of approximately 1 cm^2 are taken from each catalyst. For better resolution the samples are prepared by coating the washcoat and substrate with a 3 nm over-layer of gold.

BET surface area measurements are performed under flowing conditions using a microreactor, which has been previously described in detail elsewhere [18,19]. Approximately 0.2 g of catalyst sample is obtained from a catalyst core. The sample, containing washcoat and substrate, is crushed and sifted through a 500 μm sieve and held in place with quartz wool in a U-tube

reactor submerged in liquid nitrogen. The BET adsorption isotherm is obtained by performing Ar adsorption experiments using a mixture of Ar and He with different Ar concentrations varying from 1.5 to 7.5%. Mass 40 m/z is analyzed with the mass spectrometer in order to determine the quantity of adsorbed and desorbed Ar at each concentration.

To investigate the bonding nature of the aluminum atoms, solid state magic angle spinning (MAS) NMR was employed. These experiments were carried out on a Bruker Avance 400 (B_0 = 9.4 T) spectrometer at a resonance frequency of 104.2 MHz and spinning speed of 10 kHz. ^{27}Al 3QMAS NMR spectra were acquired using a z-filtered 3QMAS pulse sequence with optimized p1 = 4.0, p2 = 1.4, p3 = 40 μs and a recycle delay of 1.0 s [20]. Chemical shifts are referenced to 1.0 M $Al(NO_3)_3$: δ = 0 ppm. The fresh and aged Fe–zeolite/cordierite samples (20–26 mg) were obtained by scraping the zeolite washcoat from the cordierite substrate and grinding this material into a fine powder.

3. Results and discussion

3.1. Accelerated thermal aging on the engine bench

Typical temperature profiles in the emissions control system during accelerated engine-aging are shown in Fig. 3. These temperature profiles of the exhaust gases during the DPF regeneration step are repeatable for each aging temperature. In general the gas temperature at the inlet of the SCR catalyst is higher than that at the SCR exit. The difference in the gas temperature across the SCR is approximately 100 °C at 650 and 750 °C, and 50 °C at 850 °C. Since the front of the SCR is exposed to higher temperatures than the rear, it is expected that the front of the SCR catalyst will be more degraded than the rear. Due to experimental complications associated with disintegration of the vermiculite wrapping that holds the SCR catalyst in its casing, it was not possible to age each sample for the same number of cycles at each aging temperature. At 650 and 750 °C, aging was carried out for 31 and 50 cycles, respectively, but at 850 °C only 13 cycles were completed before the detritus from the vermiculite wrapping plugged the DPF.

3.2. Impact of aging on performance

After accelerated engine-aging, the catalysts are sectioned into front and rear halves before being evaluated on the bench-flow reactor with the simulated exhaust gases consisting of 5% H_2O, 5% CO_2, 14% O_2, 350 ppm NO and 350 ppm NH_3 ($\alpha = NH_3/NO_x = 1$). Fig. 4 shows NO_x conversion of fresh and accelerated engine-aged SCR catalysts as a function of evaluation temperature. The most striking feature is the drastic reduction in the NO_x performance of the front sections of the engine-aged SCR catalysts above 300 °C. The front section of the SCR catalyst engine-aged at 850 °C exhibits the worst NO_x performance followed by the catalysts engine-aged at 650 and 750 °C. The degradation in the NO_x performance is less severe in the rear sections of the engine-aged SCR catalysts at aging temperatures of 650 and 750 °C—a decrease in NO_x conversion of less than 16%. However, exposure to 850 °C results in a more significant degradation as the NO_x conversion does not exceed 50%. The results observed in the rear section of the accelerated engine-aged catalysts were similar to those reported in earlier hydrothermally-aged SCR studies [14–16].

To ensure that our results were in line with in-use SCR samples, we evaluated the front and rear sections of field-aged samples in the bench-flow reactor. Fig. 5 compares the NO_x performance of these field-aged samples to the catalysts engine-aged at 750 °C for 50 aging cycles—which is accomplished in less than 50 h. The front and rear sections of these two aged samples show the same trends

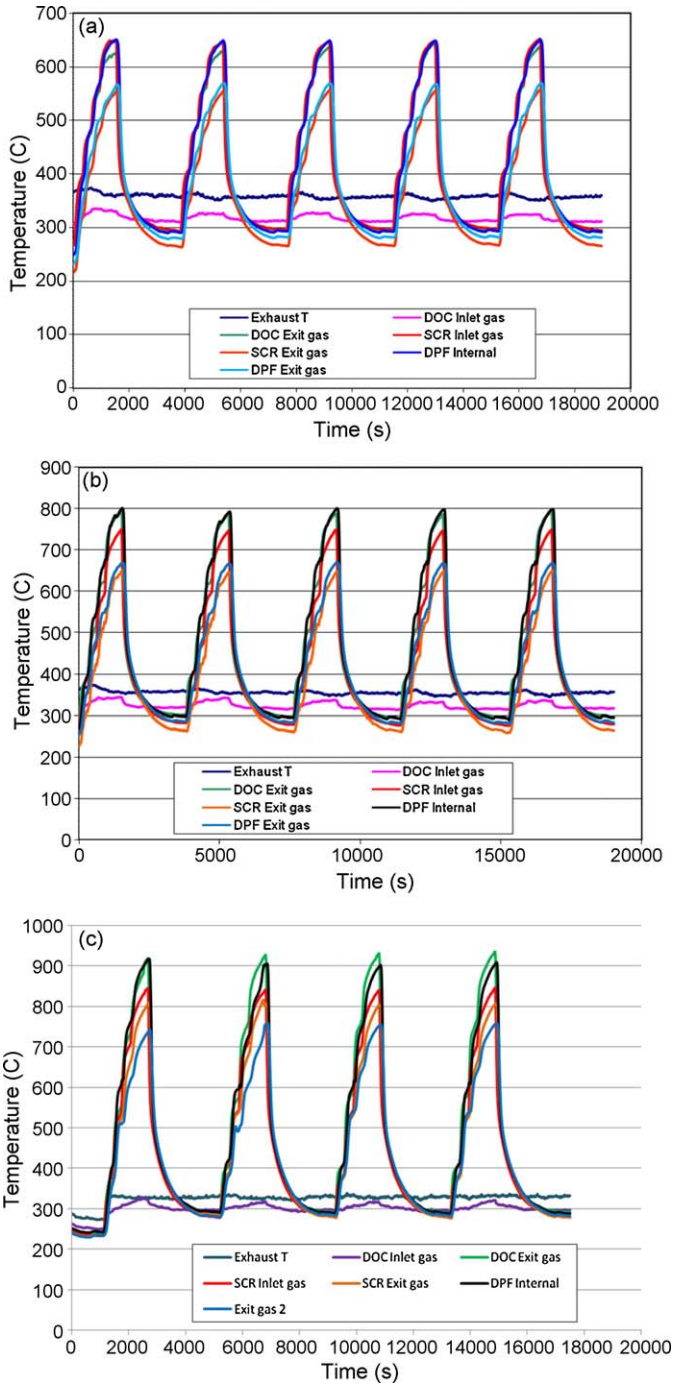

Fig. 3. Emissions control system temperatures during accelerated thermal aging on engine bench at (a) 650 °C, (b) 750 °C and (c) 850 °C.

in NO_x conversion and are similar in magnitude. This comparison, in addition to the results in Fig. 4, demonstrates that accelerated engine-aging at 650–750 °C can approximate long-term SCR aging conditions, but engine-aging to 850 °C results in conditions that are too harsh and accelerate the aging process beyond what is reasonable.

To evaluate the Fe–zeolite SCR catalysts with the more commonly employed hydrothermal aging, fresh samples were aged in the presence of H_2O, CO_2, O_2 and SO_2 in the bench-flow reactor for 64 h at 670 °C. NO_x performance was evaluated after every 16 h of aging. Fig. 6 shows that the NO_x conversion of the hydrothermally-aged SCR catalyst was minimally affected with

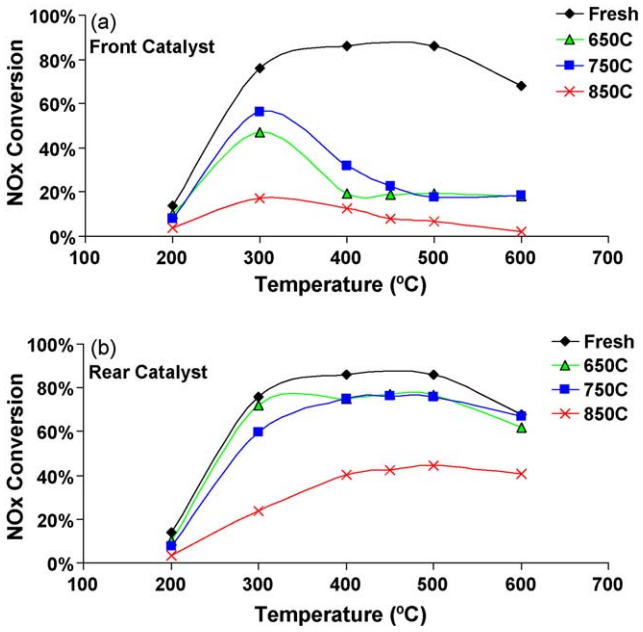

Fig. 4. NO_x conversion of the accelerated engine-aged Fe–zeolite SCR catalysts (a) front and (b) rear sections; evaluated with 5% CO_2, 5% H_2O, 14% O_2, 350 ppm NO, 350 ppm NH_3, N_2 balance, GHSV = 30,000 h^{-1}.

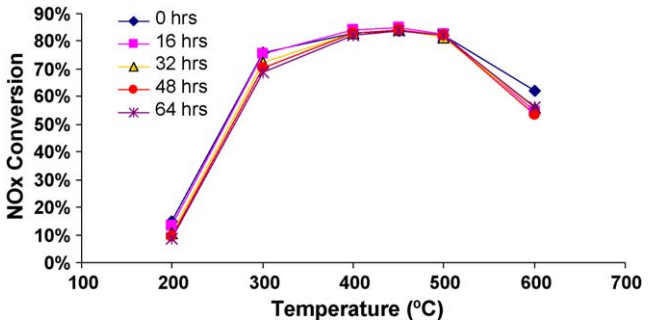

Fig. 6. Effect of temperature on NO_x conversion of the hydrothermally-aged catalyst at 670 °C; evaluated with 5% CO_2, 5% H_2O, 14% O_2, 350 ppm NO, 350 ppm NH_3, N_2 balance, GHSV = 30,000 h^{-1}.

less than a 10% decrease in NO_x conversion observed at all evaluation temperatures. Devadas et al. obtained similar results after 50 h of hydrothermal aging with a Fe–ZSM5 SCR catalyst [14]. It is apparent that bench reactor-based hydrothermal aging mimics the deactivation mechanisms observed in the rear of the engine-based systems, but the dramatic deactivation of the front sections is not captured.

3.3. Materials characterization

From the results presented up to this point it is clear that there are two deactivation mechanisms occurring in the samples. The deactivation mechanism in the front of the samples cannot be solely due to the moderately higher temperatures experienced by the front section. If this were the case then the NO_x performance of the front section of the 650 °C engine-aged sample would resemble that of the rear section of the sample aged at 750 °C, and 750 °C-front would resemble 850 °C-rear. These trends definitely do not hold true, so there must be another deactivation mechanism other than zeolite degradation/dealumination. A detailed materials characterization effort was employed in an effort to determine the deactivation mechanism responsible for the performance losses found in the front sections.

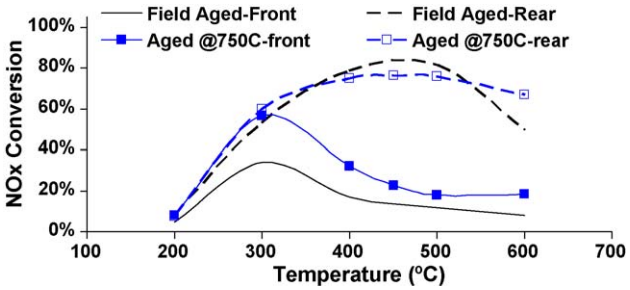

Fig. 5. NO_x conversion of the front and rear sections of the accelerated engine-aged SCR catalysts, aged at 750 °C for 50 cycles, compared to the field-aged samples; evaluated with 5% CO_2, 5% H_2O, 14% O_2, 350 ppm NO, 350 ppm NH_3, N_2 balance, GHSV = 30,000 h^{-1}.

An SEM investigation was performed to inspect the washcoat integrity in accelerated engine-aged catalysts as shown in Fig. 7. As the aging temperature increases, there are distinct differences in the washcoat appearance and adhesion to the cordierite substrate. At 650 °C (Fig. 7a), even though the samples were sectioned using a hacksaw, there is very little disturbance in either the washcoat or at the interface of the washcoat and the cordierite. This micrograph essentially duplicates that of the fresh sample. However, when aging at 750 °C (Fig. 7b), washcoat cracking and the beginning of delamination from the cordierite is visible. The damage to the washcoat is more prominent in the front section (shown) of the catalyst than the rear (not shown). This damage is even more significant in the 850 °C engine-aged sample (Fig. 7c), and there are even signs of missing washcoat from some of the channels; once again the front section displays more damage than the rear section.

While these observations from the SEM images are valuable in pointing to the escalating materials degradation at higher aging temperatures, it is more instructive when these differences are quantified. BET surface areas were measured for the fresh and engine-aged samples and are presented in Fig. 8. The values presented are based on the weights from the combination of ground washcoat and cordierite and thus are lower than the expected high surface area of zeolites. The BET measurements are generally consistent with the SEM observations and show a strong correlation between catalyst surface area and aging temperature—catalyst surface area decreases with increasing aging temperature. The surface areas of the front and rear sections of SCR catalyst engine-aged at 650 °C are 60 and 59 m^2/g, respectively, which both approximate the fresh catalyst, 58 m^2/g. At higher aging temperatures, surface areas begin to decrease and the thermal gradient is apparent as the front section is more adversely affected than the rear sample. Although it is tempting to point to these surface area differences to describe the severe deactivation in the front sections, there would have to be a notable surface area decrease in the front section of the sample aged at 650 °C to explain the results in Fig. 4. This is clearly not the case, so there must be another mechanism to explain the deactivation.

An XRD investigation was performed to study the effects of aging on the following phases in the SCR samples: iron/iron oxide, zeolite, and ceria–zirconia. Since the samples investigated were washcoated onto a cordierite monolith, which has a strong diffraction pattern with numerous features, the washcoat was scraped from the sample to minimize cordierite interference. Fig. 9 shows the XRD patterns of the fresh and accelerated engine-aged Fe–SCR catalysts; only the front sections are shown. There were only small differences detected between the front and rear sections, as would be expected with a higher temperature in the

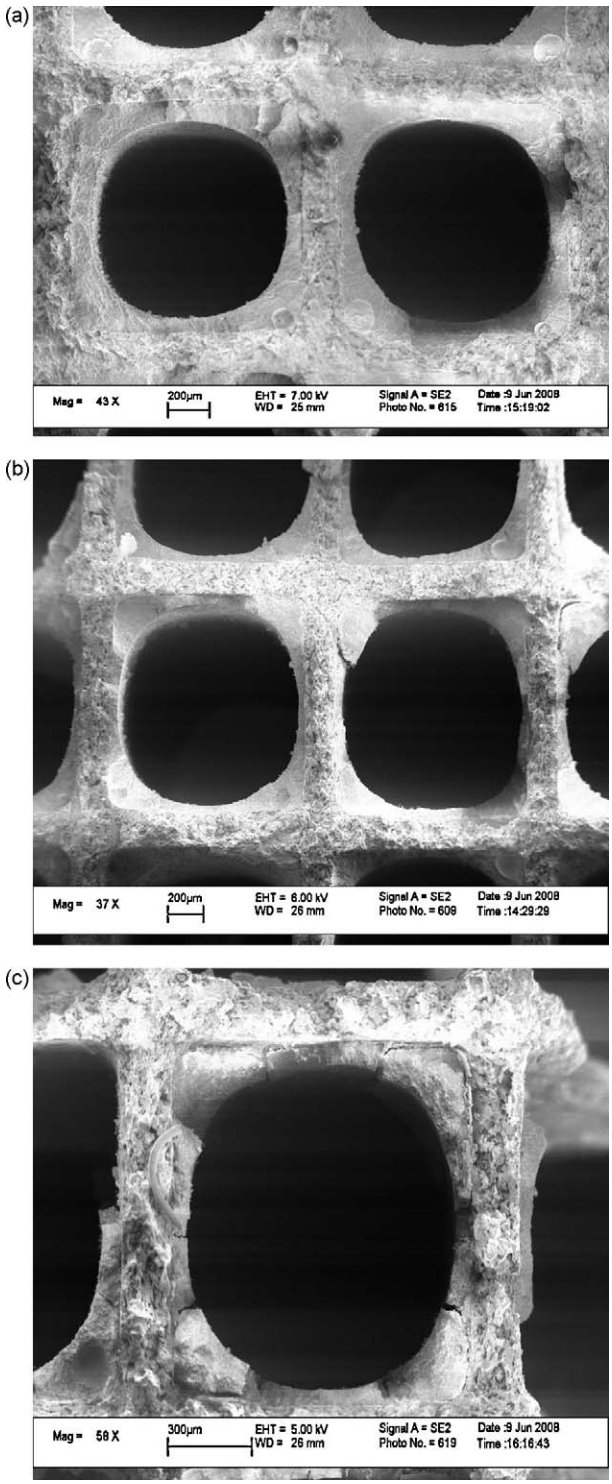

Fig. 7. SEM micrographs of Fe–zeolite SCR catalyst for the front sections of the accelerated engine-aged samples at (a) 650 °C, (b) 750 °C and (c) 850 °C.

front; however, there was not a significant phase transformation that would explain the major deactivation in the front sections. Despite our best intentions, each sample did contain a small amount of cordierite (as can be noted by the sharp peaks at $2\theta = 10.5^\circ$, 18.5°, 21.5°, 26.5°, and 28.5°), but not so much as to overwhelm the other phases. There are three main features that illustrated the phase changes that occur during the thermal aging. The clearest phase change that occurs is the gradual loss in the

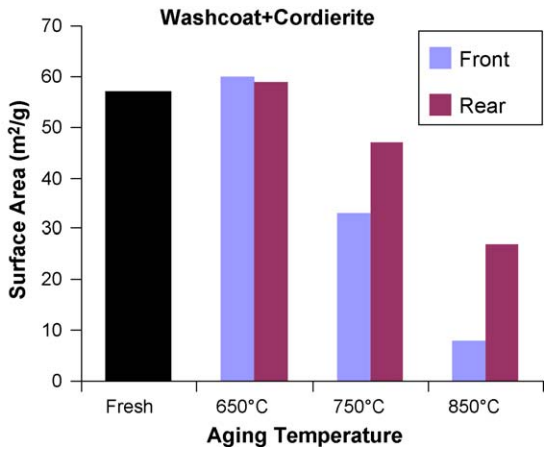

Fig. 8. BET surface area measurements of fresh and accelerated engine-aged Fe–zeolite SCR catalysts.

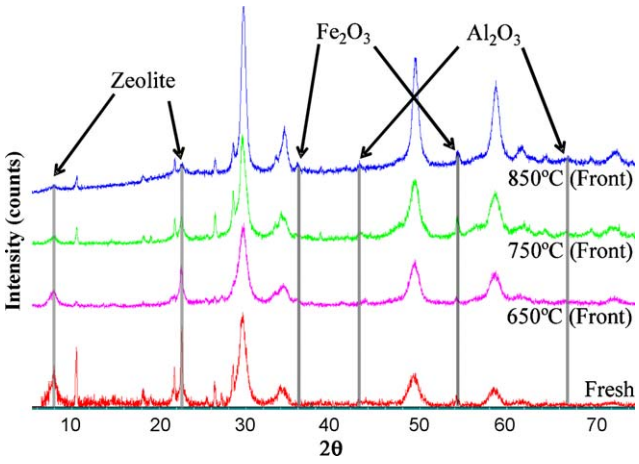

Fig. 9. X-ray diffraction patterns of fresh and accelerated engine-aged Fe–zeolite SCR catalysts.

zeolite crystallinity at increasing aging temperatures. The primary zeolite peaks are visible at $2\theta = 8^\circ$ and 22.5°. The peaks are clear and predominant in the fresh sample, and also after aging at 650 °C. However, upon heating to 750 and 850 °C the zeolite structure begins to diminish. This breakdown of the silicon and aluminum bonds generally results in alumina formation with detectable peaks of alumina in the XRD patterns occurring at $2\theta = 43^\circ$ and 67°. These peaks are more discernable at 850 °C and to a lesser extent at 750 °C. Additionally, at higher aging temperatures, there is a minor growth in the Fe_2O_3 phase at $2\theta = 36^\circ$ and 54°. This indicates that active Fe cations in the fresh catalyst have formed Fe_2O_3 clusters in the aged samples. According to Park et al., as the zeolite structure collapses, active cations are freed and they can form oxide clusters such as Fe_2O_3. As the zeolite structure begins to decompose the surface area decreases, and there will be fewer available sites to bind the Fe cations, and thus the Fe_2O_3 phase will become more prevalent [9].

Although XRD is a great tool to detect the major phase changes that are occurring, solid state ^{27}Al NMR is sensitive to the local structure and bonding and provides a method to extend our description of aluminum bonding in these heterogeneous, amorphous materials [21]. In particular the 2D experiment that employs triple quantum excitation/evolution and magic angle spinning (3QMAS) has shown great promise in resolving multiple tetrahedral and octahedral aluminum sites as well as penta-coordinate aluminum in zeolites [22].

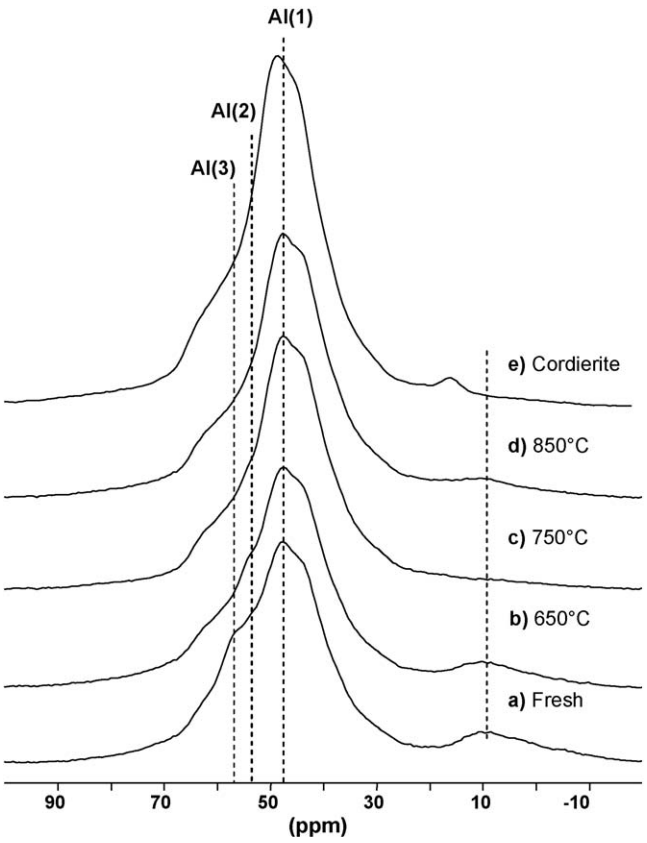

Fig. 10. One-dimensional ^{27}Al MAS spectra of the (a) fresh Fe–zeolite/cordierite, samples aged at (b) 650 °C, (c) 750 °C, and (d) 850 °C, and (e) cordierite.

The suite of stacked ^{27}Al MAS spectra in Fig. 10 are of the fresh Fe–zeolite/cordierite (a), samples aged at 650 °C (b), 750 °C (c), and 850 °C (d), and cordierite (e). The same sample suite yields the 3QMAS spectra shown in Fig. 11. In both figures the catalyst spectra are also compared with the spectrum of the support, cordierite. Cordierite and Fe–zeolite are constructed of aluminum with tetrahedral coordination represented by the asymmetric resonance band centered at 50 ppm in the 1D spectrum. The number of distinct aluminum sites is difficult to assess from the 1D data. The 2D spectrum of the fresh Fe–zeolite/cordierite, Fig. 11a, clearly shows the broad tetrahedral resonance contains three partially resolved resonances. The Al(1) resonance is due to the support (see Fig. 11e). The Al(2) and Al(3) resonances near 55 ppm arise from the Fe–zeolite catalyst [23]. These signals diminish in the successively aged samples, as seen in both Figs. 10 and 11. This dealumination has been observed in Fe–zeolites that undergo thermal treatment in air or steam [23]. The loss of the signal is attributed to dislodgement of lattice aluminum species to extra-framework positions, perhaps yielding undefined resonances due to the presence of paramagnetic iron species.

3.4. Pt identification and NH_3 oxidation

Even after this extensive materials characterization, a satisfactory explanation of the deactivation in the front section has not yet been determined. However, a similar engine-based study was recently performed by Jen et al. [24,25], and they have concluded Pt contamination in the front section of the SCR catalysts is responsible for the severe reduction in NO_x reduction performance. The DOC contains Pt and when introducing an exotherm across this device, a very small trace of the precious metal is volatilized (circa 20 ppm) and deposits on the cooler SCR. Pt is very active for NH_3

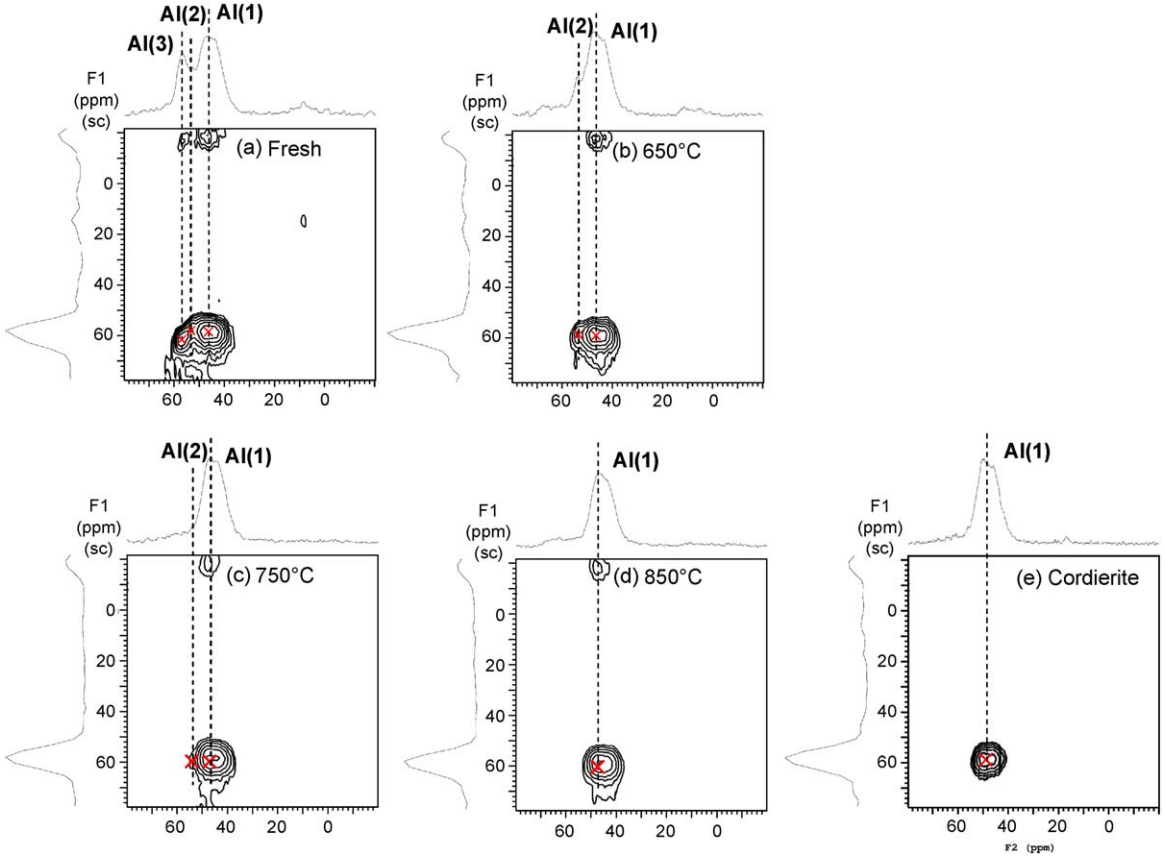

Fig. 11. Two-dimensional 3QMAS ^{27}Al NMR spectra of (a) fresh Fe–zeolite SCR catalysts and samples aged at (b) 650 °C, (c) 750 °C, and (d) 850 °C. (e) A cordierite spectrum was also recorded since it was present in each of the samples.

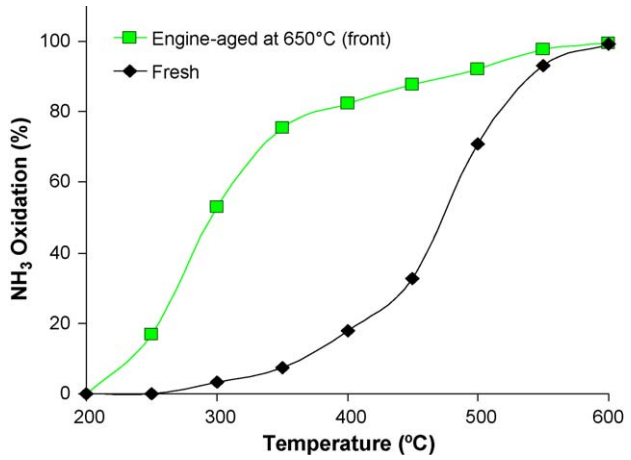

Fig. 12. NH_3 oxidation evaluated with 5% CO_2, 5% H_2O, 14% O_2, 350 ppm NH_3, N_2 balance, and a GHSV = 30,000 h^{-1}.

oxidation, such that a significant amount of the reductant will be oxidized to either NO or N_2, and thus the SCR NO_x reduction reaction cannot take place. Additional experiments to measure the rate of NH_3 oxidation in the absence of NO were performed in a bench-flow reactor that was equipped with an FTIR (Fourier Transform Infra-Red) spectrometer for NH_3 measurements. Fig. 12 illustrates this dramatic NH_3 oxidation effect for the front section of the 650 °C engine-aged sample. At 300 °C, over 50% of the NH_3 is being directly oxidized and is not available for NO_x reduction. In the fresh sample this high level of NH_3 conversion does not occur until above 500 °C. In both cases it is above this 50% threshold that the overall NO_x conversion begins to decrease (Fig. 4a).

Another interesting feature that is revealed in this NH_3 oxidation comparison is the product selectivity differences between the fresh sample and the Pt-contaminated sample, Fig. 13a and b, respectively. The first notable feature is that there is N_2O formation in the sample with Pt. This is an expected product from Pt-catalyzed NH_3 oxidation and can be used to detect potential Pt contamination in future efforts. Another expected

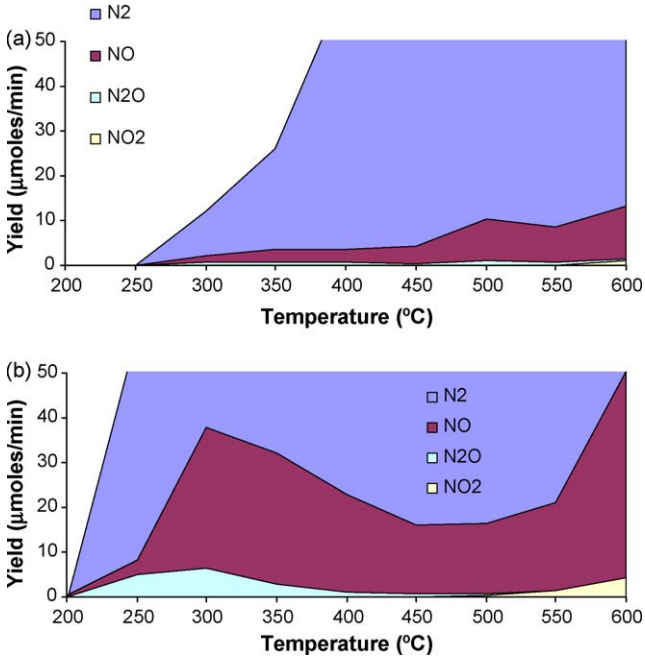

Fig. 13. Product yield during the NH_3 oxidation evaluation depicting N_2, NO, N_2O, and NO_2 in (a) fresh SCR catalyst and (b) SCR catalyst engine-aged at 650 °C.

product of Pt-catalyzed NH_3 oxidation is NO, which follows a peculiar trend in the engine-aged sample, Fig. 13b. At 300 °C the NO yield peaks, then decreases until 500 °C, where it once again begins to increase. This behavior seems to indicate the plug-flow nature of the bench-core reactor under these $NH_3 + O_2$ conditions. The NH_3 that is oxidized to NO at the inlet of the reactor, where trace Pt is located, reacts with the remaining unoxidized NH_3 following typical SCR kinetics in the back portions of the catalyst. At 300 °C, the kinetics of the SCR reaction are slow enough that a portion of the NO flows through the reactor without reacting. This then decreases between 350 and 550 °C, where the SCR kinetics are adequately high to reduce the NO that has formed from Pt-catalyzed NH_3 oxidation. Above 550 °C, the NO begins to rise sharply on the Pt-contaminated sample, which occurs because there is no longer an adequate supply of NH_3 remaining to reduce NO. It should be noted that even the fresh samples discussed here have very high NH_3 oxidation behavior. This is primarily due to the presence of ceria in the washcoat in addition to the Fe–zeolite.

4. Conclusions

Accelerated engine-aging on Fe–zeolite SCR catalysts has been carried out using a single-cylinder diesel engine fitted with an emissions control system, consisting of an upstream DOC, a Fe–zeolite SCR catalyst and a downstream DPF. Aging at SCR inlet temperatures of 650, 750 and 850 °C results in two distinct deactivation mechanisms—one that is only observed in the front section of the catalyst and one that is prevalent throughout the samples. The front-half sections of the engine-aged catalysts show significant catalyst degradation in NO_x performance at all aging temperatures. It has been determined that, during the generation of the exotherm, a portion of the Pt in the DOC volatilized and deposited on the front section of the SCR catalyst. This Pt catalyzes NH_3 oxidation, reducing the amount of reductant available for NO_x reduction. In addition to this deactivation mechanism, general zeolite degradation/dealumination was observed. This mechanism was significantly accelerated at 850 °C and resulted in significant performance losses. In comparing the results from our accelerated engine-aging to field-aged deactivation, the accelerated efforts at 750 °C appears to replicate the magnitude and general shape of the field-aged samples. This replication was achieved in less than 50 h of operation compared to the 2 years of continuous service in the field-aged catalyst.

Acknowledgements

This majority of this work was funded by the U.S. Department of Energy (DOE), Office of Energy Efficiency and Renewable Energy, Vehicle Technologies Program. The fresh and field-aged Fe–zeolite SCR catalysts were provided by Svetlana Iretskaya of Catalytic Solutions, Inc. The XRD measurements and analysis were sponsored by the Assistant Secretary for Energy Efficiency and Renewable Energy, Office of Vehicle Technologies, as part of the High Temperature Materials Laboratory (HTML) User Program. The NMR efforts were sponsored in part by the Division of Chemical Sciences, Geosciences, and Biosciences, Office of Basic Energy Sciences. Oak Ridge National Laboratory operates under DOE contract number DE-AC05-00OR22725 and is managed by UT-Battelle.

References

[1] X. Feng, W.K. Hall, J. Catal. 166 (1997) 368.
[2] M. Koebel, M. Elsener, M. Kleemann, J. Catal. 180 (1998) 171.
[3] H.Y. Chen, W.M.H. Sachtler, Catal. Lett. 50 (1998) 125.
[4] H.Y. Chen, W.M.H. Sachtler, Catal. Today 42 (1998) 73.
[5] R.M. Heck, Catal. Today 53 (1999) 519.

[6] R.Q. Long, R.T. Yang, J. Catal. 188 (1999) 332.
[7] M. Koebel, M. Elsener, M. Kleemann, Catal. Today 59 (2000) 33.
[8] Q. Sun, Z.X. Gao, H.Y. Chen, W.M.H. Sachtler, J. Catal. 201 (2001) 89.
[9] R.Q. Long, R.T. Yang, Catal. Lett. 74 (2001) 201.
[10] R.Q. Long, R.T. Yang, Catal. Lett. 207 (2002) 224.
[11] B.R. Wood, J.A. Reimer, A.T. Bell, J. Catal. 209 (2002) 151.
[12] G. Cavataio, J. Girard, J.E. Patterson, C. Montreuil, Y. Cheng, C.K. Lambert, SAE 2007-01-1575, 2007.
[13] J.R. Theis, SAE 2008-01-0811, 2008.
[14] M. Devadas, O. Krocher, A. Wokaun, React. Kinet. Catal. Lett. 86 (2) (2005) 347.
[15] M. Devadas, O. Krocher, M. Elsener, A. Wokaun, G. Mitrikas, N. Soger, M. Pfeifer, Y. Demel, L. Mussmann, Catal. Today 119 (1) (2007) 137.
[16] K. Rahkamaa-Toloen, M.L. Maunula, M. Huuhtanen, R.L. Keiski, Catal. Today 100 (3–4) (2005) 217.
[17] K. Nguyen, H.-Y. Kim, B.G. Bunting, T.J. Toops, C. Yoon, SAE 2007-01-0470, 2007.
[18] N.A. Ottinger, K. Nguyen, B.G. Bunting, T.J. Toops, J. Howe, SAE 2009-01-0634, 2009.
[19] Y. Ji, T.J. Toops, M. Crocker, Catal. Lett. 119 (2007) 257.
[20] J.-P. Amoureux, C. Fernandez, S. Steuernagel, J. Magn. Reson. A 123 (1996) 116.
[21] M.E. Smith, Appl. Magn. Reson. 4 (1993) 1.
[22] J. Huang, Y. Jiang, V.R.R. Marthala, B. Thomas, E. Romanova, M. Hunger, J. Phys. Chem. C 112 (2008) 3811.
[23] J. Perez-Ramirez, J.C. Groen, A. Bruckner, M.S. Kumar, U. Bentrup, M.N. Debbagh, L.A. Villaescusa, J. Catal. 232 (2005) 318.
[24] H.W. Jen, J.W. Girard, G. Cavataio, M.J. Jagner, SAE 2008-01-2488, 2008.
[25] G. Cavataio, H.W. Jen, J.W. Girard, M.J. Jagner, SAE 2009-01-2488, 2009.